EPJ manuscript No.
(will be inserted by the editor)

Towards a quantum gas of polar RbCs molecules

H. W. Cho[a], D. J. McCarron[a], D. L. Jenkin, M. P. Köppinger, and S. L. Cornish.

Department of Physics, Durham University, Rochester Building, Science Laboratories, South Road, Durham, DH1 3LE, United Kingdom

Received: date / Revised version: date

Abstract. We report the production of a high phase-space density mixture of ^{87}Rb and ^{133}Cs atoms in a levitated crossed optical dipole trap as the first step towards the creation of ultracold RbCs molecules via magneto-association. We present a simple and robust experimental setup designed for the sympathetic cooling of ^{133}Cs via interspecies elastic collisions with ^{87}Rb. Working with the $|F = 1, m_F = +1\rangle$ and the $|3, +3\rangle$ states of ^{87}Rb and ^{133}Cs respectively, we measure a high interspecies three-body inelastic collision rate $\sim 10^{-24}$ cm^{6}s^{-1} which hinders the sympathetic cooling. Nevertheless by careful tailoring of the evaporation we can produce phase-space densities near quantum degeneracy for both species simultaneously. In addition we report the observation of an interspecies Feshbach resonance at 181.7(5) G and demonstrate the creation of Cs_2 molecules via magneto-association on the 4g(4) resonance at 19.8 G. These results represent important steps towards the creation of ultracold RbCs molecules in our apparatus.

1 Introduction

Ultracold molecular quantum systems offer many new and exciting directions of scientific research [1]. Theoretical proposals for these systems range from precision metrology [2] and ultracold chemistry [3] to simulations of many-body quantum systems [4]. Within this field polar molecules are currently a subject of significant interest. Such molecules possess permanent electric dipole moments which give rise to anisotropic, long range dipole-dipole interactions. These interactions differ greatly from the isotropic, short-range contact interaction commonly encountered in quantum degenerate atomic gases. The orientation of these dipoles can be controlled by applying an external electric field. This control, in combination with control of the trapping geometry, enables the interactions within the quantum system to be tuned with exquisite sensitivity and may be used to suppress inelastic collisions [5]. When loaded onto an optical lattice the long-range interaction of these dipoles leads to a rich spectrum of quantum phases [6] and offers potential applications for quantum information processing [7] and simulation [8].

Realising an ultracold quantum gas of polar molecules is challenging, in part due to the complex internal structure that makes molecules interesting. This complexity is due to additional rotational and vibrational degrees of freedom and renders standard laser cooling techniques ineffective for the majority of molecules. Experimental approaches towards the creation of a quantum degenerate gas of polar molecules have mostly followed two routes.

The first approach involves the direct cooling of ground-state polar molecules. This has led to the development of many new experimental techniques [1], including Stark deceleration [9] and buffer gas cooling [10]. Typically these methods have only attained final temperatures in the millikelvin regime and phase-space densities far from degeneracy. Further advances in direct cooling will probably require the development of sympathetic cooling [11] or laser cooling [12,13].

The second approach uses the powerful laser cooling techniques applicable to atoms and starts with a high phase-space density atomic gas. Atom pairs are then associated into ground state molecules via an appropriate photoassociation scheme in which the molecular binding energy is removed by a photon [14]. The challenge of this indirect approach is to find an efficient scheme in which the population is transferred into a single target molecular state without any heating of the sample. In recent years there have been a large number of successes using the indirect approach and several schemes have produced molecules in their rovibrational ground state [15–18]. Of particular significance are two experiments that have produced ground state molecular samples close to quantum degeneracy in KRb [19] and Cs_2 [20,21]. These experiments follow a two step scheme in which weakly bound molecules are first made via magneto-association using a Feshbach resonance [22]. The resulting Feshbach molecules are then transferred into the rovibrational ground state using stimulated Raman adiabatic passage (STIRAP) [23]. The efficiency of this transfer can be enhanced using the magnetic field to tune the character of the weakly bound Feshbach molecule. Although this approach is limited to molecules whose constituent atoms can be laser cooled,

Send offprint requests to: s.l.cornish@durham.ac.uk

[a] These authors contributed equally to this work.

near 100 % conversion efficiency is possible with little heating of the gas.

Here we report our progress towards the production of ultracold polar RbCs molecules following this scheme. The success of this approach hinges on three important steps: 1. The production of a high phase-space density sample of the constituent atoms. 2. The magneto-association of weakly bound molecules via a Feshbach resonance. 3. The optical transfer of the molecules into the rovibrational ground state via STIRAP. The majority of this paper describes how the first step is achieved. Our experimental setup and cooling procedure are presented in sections 2 and 3 respectively. We then detail our progress towards the magneto-association of RbCs Feshbach molecules. In Section 4 we present the observation of a suitable interspecies Feshbach resonance and in Section 5 we demonstrate the creation of Cs_2 molecules to test the experimental protocol. A summary of the results of the paper and an outlook towards the production of RbCs molecules in the rovibrational ground state is then given in the final section.

2 Experimental Overview

The experimental setup is designed to simultaneously trap ^{87}Rb and ^{133}Cs in their absolute internal ground states. The heart of the setup consists of a levitated crossed dipole trap [24] located at the centre of an ultrahigh vacuum (UHV) glass cell. This trapping potential consists of two intersecting laser beams, a magnetic field gradient from an anti-Helmholtz coil pair and a uniform bias field from a Helmholtz coil pair. The magnetic gradient is set to 31.1 G cm^{-1} to cancel gravity and the bias field offsets the field zero position to below the crossed dipole trap such that high field seeking states are levitated. Fig. 1 presents a schematic overview of the experimental geometry. The optical contribution to the potential is provided by a 30 W IPG fibre laser with a wavelength of 1550 nm. Two 6 W beams are focussed using lenses with 200 mm focal lengths to waists of ~ 60 μm. This setup creates a trapping potential 90 μK (125 μK) deep for ^{87}Rb (^{133}Cs) and therefore permits the sympathetic cooling of ^{133}Cs via ^{87}Rb in the dipole trap. Magnetic field coils are mounted in a coil assembly centred around the glass cell, see Fig. 1. The coils are wound from square cross-section copper tubing and are water cooled. This enables currents exceeding 400 A to be applied with no adverse heating effects. These high currents allow tight magnetic confinement and large bias fields, in excess of 1150 G, to be applied.

This setup is highly versatile and can create several useful trapping potentials. By blocking one dipole beam a single beam dipole trap can be employed with axial confinement provided by the magnetic quadrupole field [25], although this potential can only trap low-field seeking states. In contrast, a two beam crossed dipole trap can confine all spin-states and allows the magnetic field to become a free parameter which can be used to tune intra- and interspecies interactions. To align the crossed dipole trap the position of each individual beam was optimised in the combined magnetic and optical potential configuration [24,25]. Both beams were positioned ~ 80 μm below the field zero of the magnetic quadrupole potential.

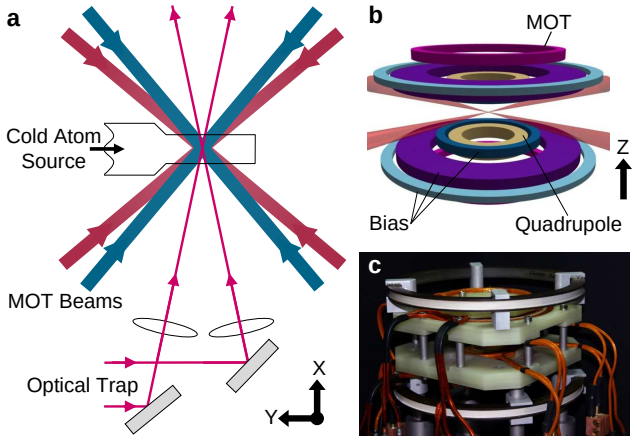

Fig. 1. Schematic of the experimental setup. (a) Optical beam layout showing the paths of the MOT beams and the beams used to make the crossed dipole trap, intersecting in the centre of a UHV glass cell. The cell is located at the centre of the magnetic coil assembly shown in (b) and (c). The assembly contains two anti-Helmholtz coils pairs for the operation of the MOT and quadrupole trap. A further three coils pairs in Helmholtz configuration can be used to create a uniform bias field at the position of the atoms.

Ultracold atomic mixtures of ^{87}Rb and ^{133}Cs are collected in an UHV glass cell using a two-species 6 beam MOT. This is fed from a two-species pyramid MOT. The atoms are prepared into the ^{87}Rb $|F = 1, m_F = -1\rangle$ and the ^{133}Cs $|F = 3, m_F = -3\rangle$ states and loaded into a magnetic quadrupole trap at 40 G cm^{-1}. Up to $6(1) \times 10^8$ ^{87}Rb and $3(1) \times 10^8$ ^{133}Cs atoms can loaded into the magnetic trap [26]. Active control of the ^{133}Cs atom number is achieved by monitoring the MOT fluorescence signal with feedback to the ^{133}Cs repump light level. With this technique the ^{133}Cs atom number loaded into the magnetic trap can be accurately and reproducibly varied between $2.5(5) \times 10^5$ and $3(1) \times 10^8$ atoms. Absorption imaging is used to probe the atoms and can analyse both ^{87}Rb and ^{133}Cs in one cycle of the experiment.

3 Cooling to High Phase-Space Density

In order to load the levitated crossed dipole trap the mixture is first precooled with forced RF evaporation in the quadrupole trap. To increase the elastic collision rate the magnetic trap is adiabatically compressed to 187 G cm^{-1}. In the magnetic quadrupole trap the trap depth set by the RF frequency is three times deeper for ^{133}Cs than for ^{87}Rb. This allows the selective RF evaporation of ^{87}Rb while interspecies elastic collisions sympathetically cool ^{133}Cs. This sympathetic cooling in the magnetic trap is presented in Fig. 2. The evaporation efficiency is defined

as $\gamma = -\frac{log(D_0/D)}{log(N_0/N)}$, here N_0 and D_0 are the initial atom number and phase-space density respectively, N and D are the final number and phase-space density respectively. In the magnetic trap the evaporation efficiency for ^{87}Rb alone is 2.5(2) (circular data points in Fig. 2). For the two-species sympathetic cooling case the cooling efficiencies are 1.7(1) and 10(1) for ^{87}Rb and ^{133}Cs respectively (square data points in Fig. 2). As expected the efficiency of the ^{87}Rb cooling has decreased during the sympathetic cooling compared to the single species case due to the additional heat load from the ^{133}Cs atoms. In contrast, the ^{133}Cs cooling efficiency is very high in accord with the successful demonstration of sympathetic cooling.

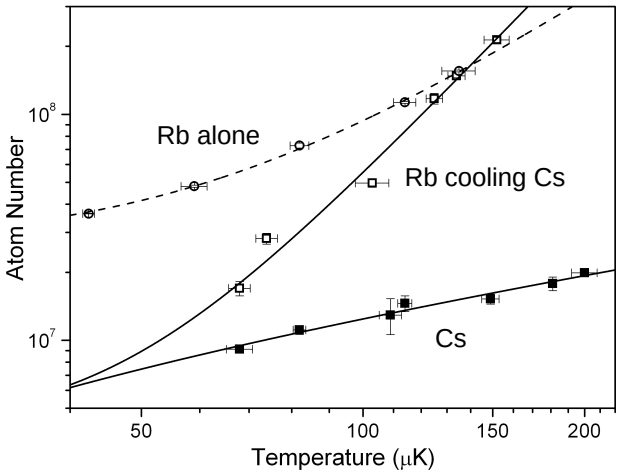

Fig. 2. Sympathetic cooling of ^{133}Cs by ^{87}Rb in the magnetic trap. Forced RF evaporation is used to cool ^{87}Rb while interspecies elastic collisions cool ^{133}Cs sympathetically. Open (closed) symbols show data for ^{87}Rb (^{133}Cs). Circular symbols show the evaporative cooling of ^{87}Rb alone. Square symbols show the two species sympathetic cooling case.

Once the mixture is cooled below ~ 70 μK Majorana spin-flip losses start to limit the efficiency of any further cooling in the magnetic trap. At this point the crossed dipole trap is loaded by simply reducing the magnetic field gradient to 29.0 G cm^{-1}, slightly below the 31.1 G cm^{-1} required to exactly levitate the atoms. Further benefits of interspecies elastic collisions are observed when loading the dipole trap. By carefully selecting the composition of the mixture and the final frequency of the RF applied during the load, up to 50 % of the ^{133}Cs can be transferred into the dipole trap. This is double the number of atoms loaded compared to the ^{133}Cs alone case. We believe this enhancement results from elastic collisions with the ^{87}Rb atoms and indicates a large interspecies elastic cross-section. Once in the levitated crossed dipole trap the phase-space densities are $1.3(1)\times10^{-3}$ and $5.8(5)\times10^{-4}$ for ^{87}Rb and ^{133}Cs respectively. This represents a significant increase from the phase-space densities in the quadrupole trap. This arises because the transfer is analogous to forced evaporation; here the 'evaporated' atoms are in the low-density tails of the weak quadrupole trap. Immediately after loading the dipole trap the atomic spins of the mixture are adiabatically flipped into $|F = 1, m_F = +1\rangle$ for ^{87}Rb and $|F = 3, m_F = +3\rangle$ for ^{133}Cs, and a 22.8 G bias field is applied [24]. This transfer to the absolute ground states means that inelastic two-body losses are avoided. At 22.8 G the ratio of elastic to three-body inelastic collisions in ^{133}Cs is favourable for the production of Bose-Einstein condensates [27].

After loading the crossed dipole trap the atomic densities are $\approx 5\times10^{12}$ cm^{-3} for ^{87}Rb and $\approx 10^{12}$ cm^{-3} for ^{133}Cs. When both ^{87}Rb and ^{133}Cs are present in the trap at these high densities very strong interspecies inelastic losses are observed, see Fig. 3. The observed lifetimes of the minority species at short times are consistent with interspecies three-body loss rate coefficients of $\sim 10^{-24}$ cm^6 s^{-1}. Such strong inelastic losses are a major hurdle when trying to achieve a high phase-space density mixture of ^{87}Rb and ^{133}Cs as they cause both atom loss and heating.

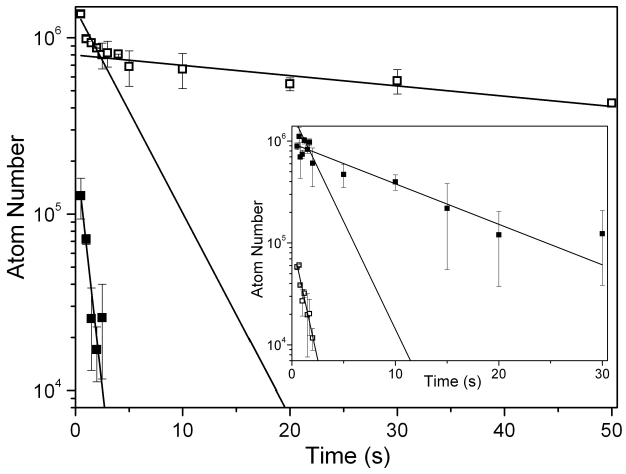

Fig. 3. Interspecies three-body loss in the crossed dipole trap. Open (closed) symbols show data for ^{87}Rb (^{133}Cs). The data are fit with a double exponential function to determine trap lifetimes. In the main plot ^{133}Cs is the minority species and the lifetimes are ^{133}Cs $\tau = 0.8(1)$ s, ^{87}Rb $\tau_1 = 4(1)$ s, and ^{87}Rb $\tau_2 = 70(10)$ s. In the inset ^{87}Rb is the minority species and the lifetimes are ^{87}Rb $\tau = 0.9(2)$ s, ^{133}Cs $\tau_1 = 2(1)$ s, ^{133}Cs $\tau_2 = 10(3)$ s.

To combat the interspecies three-body loss in the dipole trap fast evaporative cooling is performed. By reducing both beam powers to 120 mW in 1.0 s the ^{87}Rb trap depth is reduced to 2 μK. This stage not only cools the mixture but also significantly relaxes the trap and results in the atomic density in the trap decreasing by a factor of $\sim$3. This decrease in density, and the associated decrease in the elastic collision rate, is normally viewed as detrimental for evaporative cooling, but here it is a benefit. As a result the observed dual species mixture lifetime in the trap increases by approximately one order of magnitude. The evaporation efficiencies for this ramp in the dipole trap are 1.9(1) and 2.4(1) for ^{87}Rb and ^{133}Cs respectively. After this cut the mixture consists of $4.7(1)\times10^5$ ^{87}Rb

atoms and $1.5(1) \times 10^5$ ^{133}Cs atoms at 0.32(1) μK, corresponding to phase-space densities of 0.053(1) and 0.021(1) for ^{87}Rb and ^{133}Cs respectively. The final trap lifetime of the minority species (^{133}Cs) is 8(2) s. The trajectory to a high phase-space density mixture of ^{87}Rb and ^{133}Cs is summarised in Fig. 4.

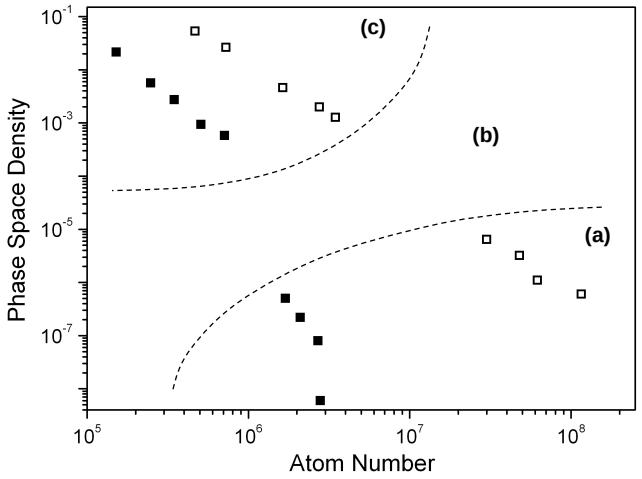

Fig. 4. Trajectory to high phase-space density for a mixture of ^{87}Rb and ^{133}Cs. Open (closed) symbols show data for ^{87}Rb (^{133}Cs). The trajectory is divided into three sections: (a) RF evaporation and sympathetic cooling in the magnetic trap, (b) loading the levitated crossed dipole trap, and (c) evaporative cooling in the levitated crossed dipole trap.

4 Interspecies Feshbach Resonance

Once a high phase-space density ^{87}Rb ^{133}Cs mixture has been made in the levitated crossed dipole trap the search for interspecies Feshbach resonances can begin. Feshbach resonances are most easily detected through an enhancement of trap loss [28]. To increase the sensitivity of heteronuclear Feshbach spectroscopy a significant imbalance between the two-species atom numbers is useful [29]. Here the majority species acts as a collisional bath for the minority species which is used as a probe. If the atom number imbalance is large the probe species will be significantly depleted when a resonance is encountered, leaving the majority species largely unchanged. In this experiment the lowest internal energy states are used, this results in trap loss being due to three-body collisions only. To perform sensitive Feshbach spectroscopy a high atomic density for both species is essential as interspecies collisions govern the loss rates from the trap. For the data presented the densities are $1.6(1) \times 10^{12}$ cm^{-3} and $3.1(4) \times 10^{11}$ cm^{-3} for ^{87}Rb and ^{133}Cs respectively. The mixture contains $3.0(3) \times 10^5$ ^{87}Rb atoms, and $2.6(4) \times 10^4$ ^{133}Cs atoms at 0.32(1) μK. Using such a low temperature ensures that only s-wave resonances can be observed during the spectroscopy. For each experimental cycle the ultracold mixture is allowed to evolve at a specific homogeneous magnetic field for 5 s, and then the ^{133}Cs atom number is measured. In Fig. 5 the detection of a Feshbach resonance near 180 G is presented, each data point corresponds to an average of 3-5 measurements.

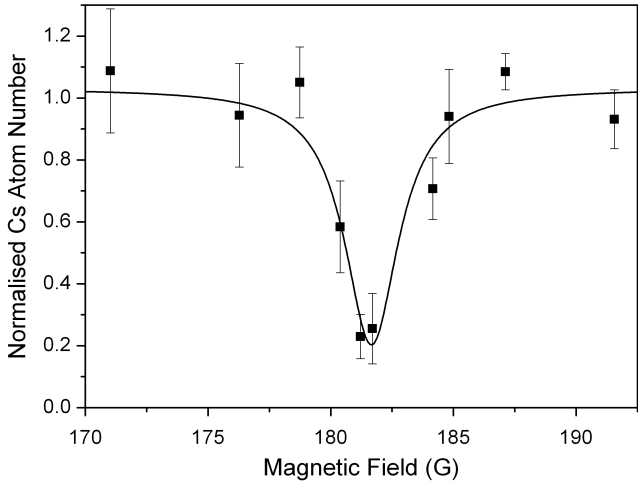

Fig. 5. Observation of an interspecies ^{87}Rb^{133}Cs Feshbach resonance using loss spectroscopy. The $|1,+1\rangle$ and $|3,+3\rangle$ states were used for ^{87}Rb and ^{133}Cs respectively. The ^{133}Cs (minority species) atom number after a 5 s hold is normalised to the corresponding mean number recorded off resonance. A Lorentzian fit is applied to the data to measure the position and width of the resonance. From the fit the resonance position $B_0 = 181.7(5)$ G, and the resonance width $\Delta B \approx 3$ G.

By fitting a Lorentzian function to the data shown in Fig. 5 the position and width of the Feshbach resonance can be measured. From the fit the resonance position $B_0 = 181.7(5)$ G, and the resonance width $\Delta B \approx 3$ G. These results are in excellent agreement with the previous measurement of this resonance [30]. Using this setup we are currently extending the interspecies Feshbach resonance search up to bias fields in excess of 1150 G, and to ^{85}Rb and ^{133}Cs mixtures. Locating an interspecies Feshbach resonance now opens the possibility of creating RbCs molecules via magneto-association.

5 Feshbach Association

The second step towards the production of ground state molecules requires the controlled magneto-association of weakly bound molecules using a Feshbach resonance. To develop experimental protocols and detection methods the magneto-association of Cs_2 dimers has been explored using a well characterised ^{133}Cs Feshbach resonance [31]. To create a high phase-space density sample of only ^{133}Cs, both ^{87}Rb and ^{133}Cs are loaded into the magnetic quadrupole trap and the standard sympathetic cooling of ^{133}Cs via ^{87}Rb is performed (see Fig. 2). However the final RF frequency is decreased to cut away all of the ^{87}Rb atoms during the loading of the dipole trap. Further evaporation is performed until the ^{133}Cs cloud is close to degeneracy.

The $|3,+3\rangle$ state used has a 4(g)4 Feshbach resonance at 19.8 G [32] that is estimated to be 5 mG wide [31]. (The 4(g)4 notation refers to the $F = 4, l = 4$ and $m_F = 4$ molecular state, where F is the total internal angular momentum, l is the rotational angular momentum, and m_F is the projection along the quantization axis.) This resonance is crossed from high to low field at a rate of 47 G s^{-1}. The field is then rapidly jumped to 17 G to null atomic interactions and the dipole trap is switched off. Stern-Gerlach separation is immediately applied to spatially distinguish between the atomic and molecular samples. The magnetic field gradient is fixed at 31.1 G cm^{-1} to levitate the atomic cloud. During this variable hold time the molecules fall down away from the levitated atoms due to their smaller magnetic moment to mass ratio. To dissociate the molecules for imaging the magnetic field is jumped back across the resonance to 21 G in 130 μs. This reverse sweep brings the molecules above the scattering continuum, from here they rapidly dissociate into free atoms. Finally the magnetic field gradient is switched off for a 2 ms free expansion before an absorption image reveals the distribution of the dissociated molecules (and the free atoms).

The atomic and molecular clouds' positions as a function of the levitation time is presented in Fig. 6. The inset to this figure shows a typical absorption image, at the top a large atom cloud is levitated while a smaller molecular cloud falls away. Typical magneto-association efficiencies are ∼12% and samples containing 7,000 molecules are produced from the high phase-space density ^{133}Cs cloud. The molecular acceleration can be measured from the data presented in Fig. 6 and this allows the magnetic moment for the Cs_2 molecules to be calculated. The molecular acceleration at 31.1 G cm^{-1} is measured to be 3.86(4) m s^{-2}, this corresponds to a magnetic moment $\mu = 0.92(1)\mu_B$. This value concurs with another measurement performed by levitating the molecular cloud at 51.4(2) G cm^{-1}. These results are in good agreement with previous work and theoretical calculations [31].

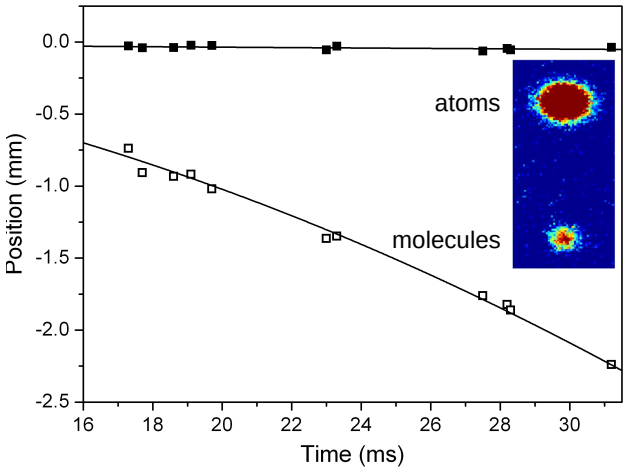

Fig. 6. The production of Cs_2 molecules using a Feshbach resonance. Open (closed) symbols mark the molecular (atomic) clouds position as a function of the levitation time. From these data a molecular acceleration of 3.86(4) m/s^2 is measured, this corresponds to $\mu = 0.92(1)\mu_B$. Inset: A typical absorption image taken after the molecules have been dissociated back into atoms. At the top the levitated atomic cloud contains 1.0×10^5 atoms, the smaller molecular sample below contained 7.5×10^3 Cs_2 Feshbach molecules.

6 Conclusion and Outlook

In this paper we have presented a simple levitated crossed dipole trap which is easily loaded from a magnetic quadrupole trap and is suitable for the sympathetic cooling of ^{133}Cs by ^{87}Rb to high phase-space densities. The simplicity of the setup and method is in contrast to previous work on ultracold mixtures of ^{87}Rb and ^{133}Cs [30]. We believe our approach could be readily implemented into many existing experimental setups that have Helmholtz and anti-Helmholtz coils already in position.

Using this simple approach we have succeeded in making a high phase-space density mixture of ^{87}Rb and ^{133}Cs combatting strong three-body losses en route through careful optimisation of the evaporative cooling. This high phase-space density mixture has the appropriate starting conditions for efficient magneto-association. With this in mind we have observed an interspecies Feshbach resonance at 181.7(5) G and have created Cs_2 dimers using a ^{133}Cs Feshbach resonance to test the experimental protocol.

The next step is to perform Feshbach association of ^{87}Rb and ^{133}Cs into weakly bound heteronuclear molecules via an interspecies Feshbach resonance. A broad entrance-channel dominated resonance such as that shown in Fig. 5 could be an ideal candidate for Feshbach association [22,28]. Exploration of the bound state spectrum close to threshold [33] should then allow the identification of a molecular state suitable for optical transfer to the rovibrational ground state. We are currently developing the STIRAP laser system, following the transfer scheme first proposed in ref. [34]. The optical excitation of the Feshbach molecules is at a wavelength of ∼ 1550 nm. The wavelength of the second photon is then selected to remove the 3836.14(50) cm^{-1} of binding energy [35] of the rovibrational molecular ground state. We expect ultracold ground state RbCs molecules to be within reach shortly in our experiments.

We acknowledge financial support by the the Engineering and Physical Sciences Research Council (grants GR/S78339/01, EP/E041604/1, EP/H03363/1), and the European Science Foundation within the framework of the EuroQUAM collaboartive research project QuDipMol. SLC acknowledges the support of the Royal Society..

References

1. L.D. Carr, D. DeMille, R.V. Krems, J. Ye, New J. Phys. **11**(5), 055049 (2009)
2. T. Zelevinsky, S. Kotochigova, J. Ye, Phys. Rev. Lett. **100**(4), 043201 (2008)

3. R.V. Krems, Phys. Chem. Chem. Phys. **10**, 4079 (2008)
4. G. Pupillo, A. Micheli, H.P. Büchler, P. Zoller, *Cold molecules: Theory, experiment, applications* (CRC Press, Boca Raton, 2009), chap. 12
5. A.V. Avdeenkov, M. Kajita, J.L. Bohn, Phys. Rev. A **73**(2), 022707 (2006)
6. B. Capogrosso-Sansone, C. Trefzger, M. Lewenstein, P. Zoller, G. Pupillo, Phys. Rev. Lett. **104**(12), 125301 (2010)
7. D. DeMille, Phys. Rev. Lett. **88**, 067901 (2002)
8. A. Micheli, G.K. Brennen, P. Zoller, Nat. Phys. **2**, 341 (2006)
9. H.L. Bethlem, G. Berden, G. Meijer, Phys. Rev. Lett. **83**(8), 1558 (1999)
10. J.D. Weinstein, R. deCarvalho, T. Guillet, B. Friedrich, J.M. Doyle, Nature **395**, 148 (1998)
11. G. Modugno, G. Ferrari, G. Roati, R.J. Brecha, A. Simoni, M. Inguscio, Science **294**, 1320 (2001)
12. B.K. Stuhl, B.C. Sawyer, D. Wang, J. Ye, Phys. Rev. Lett. **101**(24), 243002 (2008)
13. E.S. Shuman, J.F. Barry, D. DeMille, Nature **467**, 820 (2010)
14. K.M. Jones, E. Tiesinga, P.D. Lett, P.S. Julienne, Rev. Mod. Phys. **78**(2), 483 (2006)
15. J.S. Sage, S. Sainis, T. Bergeman, D. DeMille, Phys. Rev. Lett. **94**, 203001 (2005)
16. J. Deiglmayr, A. Grochola, M. Repp, K. Mörtlbauer, C. Glück, J. Lange, O. Dulieu, R. Wester, M. Weidemüller, Phys. Rev. Lett. **101**(13), 133004 (2008)
17. M. Viteau, A. Chotia, M. Allegrini, N. Bouloufa, O. Dulieu, D. Comparat, P. Pillet, Science **321**, 232 (2008)
18. F. Lang, K. Winkler, C. Strauss, R. Grimm, J.H. Denschlag, Phys. Rev. Lett. **101**(13), 133005 (2008)
19. K.K. Ni, S. Ospelkaus, M.H.G. de Miranda, A. Pe'er, B. Neyenhuis, J.J. Zirbel, S. Kotochigova, P.S. Julienne, D.S. Jin, J. Ye, Science **322**(5899), 231 (2008)
20. J.G. Danzl, E. Haller, M. Gustavsson, M.J. Mark, R. Hart, N. Bouloufa, O. Dulieu, H. Ritsch, H.C. Nägerl, Science **321**, 1062 (2008)
21. J. Danzl, M.J. Mark, E. Haller, M. Gustavsson, R. Hart, J. Aldegunde, J.M. Hutson, H.C. Nägerl, Nature Phys. **6**(5899), 231 (2010)
22. T. Köhler, K. Góral, P.S. Julienne, Rev. Mod. Phys. **78**(4), 1311 (2006)
23. K. Bergmann, H. Theuer, B.W. Shore, Rev. Mod. Phys. **70**(3), 1003 (1998)
24. D.L. Jenkin, D.J. McCarron, M.P. Köppinger, K.L. Butler, H.W. Cho, S.A. Hopkins, S.L. Cornish, in preparation (2011)
25. Y.J. Lin, A.R. Perry, R.L. Compton, I.B. Spielman, J.V. Porto, Phys. Rev. A **79**(6), 063631 (2009)
26. M.L. Harris, P. Tierney, S.L. Cornish, J. Phys. B **41**, 035303 (2008)
27. T. Weber, J. Herbig, M. Mark, H.C. Nägerl, R. Grimm, Science **299**, 232 (2003)
28. C. Chin, R. Grimm, P. Julienne, E. Tiesinga, Rev. Mod. Phys. **82**(2), 1225 (2010)
29. E. Wille, F.M. Spiegelhalder, G. Kerner, D. Naik, A. Trenkwalder, G. Hendl, F. Schreck, R. Grimm, T.G. Tiecke, J.T.M. Walraven et al., Phys. Rev. Lett. **100**(5), 053201 (2008)
30. K. Pilch, A.D. Lange, A. Prantner, G. Kerner, F. Ferlaino, H.C. Nägerl, R. Grimm, Phys. Rev. A **79**(4), 042718 (2009)
31. J. Herbig, T. Kraemer, M. Mark, T. Weber, C. Chin, H.C. Nägerl, R. Grimm, Science **301**(5639), 1510 (2003)
32. V. Vuletić, C. Chin, A.J. Kerman, S. Chu, Phys. Rev. Lett. **83**(5), 943 (1999)
33. M. Mark, F. Ferlaino, S. Knoop, J.G. Danzl, T. Kraemer, C. Chin, H.C. Nägerl, R. Grimm, Phys. Rev. A **76**(4), 042514 (2007)
34. W. Stwalley, Eur. Phys. J. D **31**, 221 (2004)
35. P.S. Żuchowski, J.M. Hutson, Phys. Rev. A **81**(6), 060703 (2010)